EXTREME LOADS OF A TRAINER JET FOLLOWING A SUDDEN DEFLECTION OF CONTROL SURFACE

Zdobyslaw Goraj, Warsaw University of Technology, goraj@meil.pw.edu.pl
Aleksander Olejnik, Military University of Technology, Warsaw, Poland

Keywords: *flight dynamics, gust, aerodynamic loads*

Abstract

Each airplane is not only operated in a level steady flight, but also has to perform a number of maneuvers. Sometimes these maneuvers are very rapid and it is the reason that extreme loads generated in such maneuvers on the tailplanes have to be calculated. These loads are responsible for the state of strain, elastic deflection, fatigue and other phenomena. Among different maneuvers considered in this paper are motions following a sudden deflection of elevator and response to a vertical gust. This paper focuses mainly on the flight dynamics and flight control system of a trainer jet aircraft. Analysis is based on the linearized equation of motion of a rigid airplane of six degrees of freedom in an arbitrary motion with deflectable control surfaces. An important point in the analysis was estimating the stability derivatives, computed by means of panel methods, and compared with the results of classical engineering approach.

1 General Introduction

The main goal of this paper is to present a quick and reliable method for computing of lifting force and pitching moment acting on an airplane in selected rapid maneuvers. Among typical maneuvers are the motions following: (1) sudden deflection of the elevator, (2) vertical gust, (3) dropping a container, (4) dropping the water from a firefighting airplane, (5) sudden flap deflection and (6) sudden change of the engine thrust. In this paper the maneuvers following a sudden deflection of elevator and a sudden vertical gust were analyzed in details. The panel methods [6,8,11] supplemented by a traditional engineering approach (see, e.g. ESDU [3]) were used to compute important aerodynamic coefficients, including lift-curve slope, zero-lift angle of attack, downwash, polar drag coefficients, pitching moment curve slope, tailplane lift-curve slopes, all versus the angle of attack and elevator deflection. The dynamic equations of disturbed motion were derived from two fundamental equations of the rigid body motion – the equation of change of momentum and the equation of change of moment of momentum. The disturbed motion is related to the state of airplane equilibrium, i.e. angle of attack increment, elevator deflection increment and all other parameter increments are equal to zero in the state of equilibrium. The aerodynamic forces and moment acting on the airplane in the disturbed state are computed as a sum of products of stability derivatives and disturbances (corresponding to the longitudinal, plunging and pitching motions, respectively). The approach used in this paper enables computing the aerodynamic and inertial forces acting on the airplane structure, and then finally the extreme states of loads, the state of strain and the fatigue wear degree. The detailed calculations were performed for X-2000, a trainer airplane.

2 List of symbols

a - wing lift-curve slope, $\partial C_{Lw}/\partial\alpha$
a_1 - tailplane lift-curve slope versus angle of attack, $\partial C_{LH}/\partial\alpha$
a_2 - tailplane lift-curve slope versus elevator deflection, $\partial C_{LH}/\partial\delta_H$
$A(A_H)$ - main wing (tailplane) aspect ratio
$C_a = MAC$ - Mean Aerodynamic Chord
C_L, C_D - lift and drag coefficients

C_m - pitching moment coefficient, around the mean quarter-chord point *A*

$C_{mwB,C}$ - pitching moment coefficient of the wing-body combination about the *CG* (for an arbitrary C_L)

$C_{mwB,0}$ - pitching moment coefficient of the wing-body combination about the *CG* for $C_L=0$

D, L, M - drag, lift and pitching moment for whole aircraft

J_y - moment of inertia about y axis

M_{Cy}, M^{T}_{Cy} - aerodynamic and thrust pitching moment of the whole aircraft about the *CG*

m - mass of the whole aircraft

n_z - normal load coefficient

P_{sx}, P_{sz} - components of thrust (along and perpendicular to *MAC)*

Q - pitch rate

S (S_H) - main wing (tailplane) area

U,W - speed components in maneuver

U_0,W_0 - speed components in steady flight

u,w - small disturbances of *U,W*

x_A , x_C , z_C , x_N - co-ordinates of points *A, C, N, H* with respect to nose of *MAC*

x_0, z_0 - co-ordinates of aircraft position in the ground fixed axis system

α_{DYN}- dynamic angle of attack (angle between vector of the airplane speed and *MAC* direction); $\alpha_{DYN}=\alpha$

α_{KIN} - kinematic angle of attack (angle between vector of the air-flow over the airplane and *MAC* direction)

α_{ST} - angle of attack in a steady flight

δ_H - elevator deflection

ε - downwash

ε_0 - downwash when $\alpha=0$

$d\varepsilon/d\alpha$ - slope of downwash versus to angle of attack

θ, ϑ - pitch angle & its small disturbance

ΔX, ΔY, ΔZ, Δu, Δw - increments of forces, pitching moment and speed in maneuver

X_u,X_w,X_q,Z_u,Z_w, …- dimensional stability derivatives

C_{Du},C_{Dw},C_{Dq},$C_{Lu,\ldots}$ - dimensionless stability derivatives

κ_H - horizontal tail volume

3 Dynamic equations of motion

The dynamic equations of motion [2] have been written for the body frame of reference Axyz and have the form:

$$\begin{aligned}
&m(\dot{U}+QW)-mz\dot{Q}+m(xQ^2)\\
&\quad =X-mg\sin\Theta+P_{sx},\\
&m(\dot{W}-QU)+mx\dot{Q}+m(zQ^2)\\
&\quad =Z+mg\cos\Theta+P_{sz},\\
&J_y+m\{x(\dot{W}-UQ)-z(\dot{U}+QW)\}\\
&\quad =M_{Ay}+M^{T}_{Ay}+mg(z\sin\Theta+x\cos\Theta),\\
&Q=\dot{\Theta},
\end{aligned} \tag{1}$$

where *x, z* denote the coordinates of the airplane center of gravity in the design frame of reference $Ax_Dy_Dz_D$ (axis Ax_D is directed along *MAC*, opposite to the flight direction; Az_D is perpendicular to Ax_D and is directed to the top of airplane).

The forces and pitching moment (present on the right side of eq.(1)) in the state of equilibrium are equal to zero. That is the reason to write the equations of motion of small disturbances with respect to the state of equilibrium. Coming from an assumption that the velocities (and path angle) consist of steady state and perturbation components we have

$$\begin{aligned}
&m[\dot{u}+q(W_0+w)]\\
&\quad =\Delta X+\frac{\partial X}{\partial u}u+\frac{\partial X}{\partial w}w+\frac{\partial X}{\partial q}q+\frac{\partial X}{\partial \dot{w}}\dot{w}\\
&\quad +mg(\cos\Theta_0\sin\vartheta),\\
&m[\dot{w}-q(U_0+u)]\\
&\quad =\Delta Z+\frac{\partial Z}{\partial u}u+\frac{\partial Z}{\partial w}w+\frac{\partial Z}{\partial q}q+\frac{\partial Z}{\partial \dot{w}}\dot{w}\\
&\quad -mg(\sin\Theta_0\sin\vartheta),\\
&J_y\dot{q}=\Delta M+\frac{\partial M}{\partial u}u+\frac{\partial M}{\partial w}w+\frac{\partial M}{\partial q}q+\frac{\partial M}{\partial \dot{w}}\dot{w},
\end{aligned} \tag{2}$$

where ΔX, ΔZ, ΔM denote increments of forces and pitching moment due to performing a maneuver (following the elevator deflection, gust or other external input).

The increments can be computed as follows:

$$\begin{aligned}
\Delta X &= X - mg\sin\Theta + P_{sx} = \\
&- D\cos\alpha + L\sin\alpha - D_H\cos(\alpha-\varepsilon) \\
&+ L_H\sin(\alpha-\varepsilon) - mg\sin\Theta + P_s\cos\varphi, \\
\Delta Z &= Z + mg\cos\Theta + P_{sz} \\
&= -L\cos\alpha - D\sin\alpha - L_H\cos(\alpha-\varepsilon) \\
&- D_H\sin(\alpha-\varepsilon) + mg\cos\Theta + P_s\sin\varphi, \\
\Delta M &= M_{Cy} + M_{Cy}^T = M_{Cy} \\
&- P_s\cos\varphi(z_S - z_C) - P_s\sin\varphi(x_S - x_C),
\end{aligned} \tag{3}$$

where

$$\begin{aligned}
&L = \tfrac{1}{2}\rho V^2 S C_L\,;\; D = \tfrac{1}{2}\rho V^2 S C_D\,, \\
&M_C = \tfrac{1}{2}\rho V^2 S C_m C_a\,, \\
&L_H = \tfrac{1}{2}\rho V^2\left(\frac{V_H}{V}\right)^2 S_H C_{LH}\,, \\
&D_H = \tfrac{1}{2}\rho V^2\left(\frac{V_H}{V}\right)^2 S_H C_{DH}\,, \\
&C_m = C_{mwB,C} - (C_{LH}\cos(\alpha-\varepsilon) \\
&+ C_{DH}\sin(\alpha-\varepsilon))\kappa_H \\
&+ (C_{DH}\cos(\alpha-\varepsilon) - C_{LH}\sin(\alpha-\varepsilon))\kappa_H\,, \\
&C_{mwB,C} = \frac{\partial C_{mwB,C}}{\partial C_L} C_L + C_{mwB,0}\,, \\
&C_L = (\alpha-\alpha_0)\frac{dC_L}{d\alpha}\,, \\
&C_D = C_{D0} + \frac{C_L^2}{\pi A}\,, \\
&C_{LH} = a_1\alpha_H + a_2\delta_H\,, \\
&C_{DH} = C_{DH0} + \frac{C_{LH}^2}{\pi A_H}\,, \\
&\kappa_H = \frac{S_H(x_{AH} - x_C)}{SC_a}\,.
\end{aligned} \tag{4}$$

The dimensional stability derivatives in Eq. (2) depend on the dimensionless stability derivatives as follows

$$\begin{aligned}
X_u &= \frac{\partial X}{\partial u} = (-2C_D - C_{Du})\tfrac{1}{2}\rho SV \\
X_w &= \frac{\partial X}{\partial w} = -C_{Dw}\tfrac{1}{2}\rho SV \\
X_q &= \frac{\partial X}{\partial q} = -C_{Dq}\tfrac{1}{2}\rho SVC_a \\
X_{\dot w} &= \frac{\partial X}{\partial \dot w} = M_u \cong 0
\end{aligned} \tag{5}$$

$$\begin{aligned}
Z_u &= \frac{\partial Z}{\partial u} = (-2C_L - C_{Lu})\tfrac{1}{2}\rho SV \\
Z_w &= \frac{\partial Z}{\partial w} = -C_{Lw}\tfrac{1}{2}\rho SV \\
Z_q &= \frac{\partial Z}{\partial q} = -C_{Lq}\tfrac{1}{2}\rho SVC_a \\
Z_{\dot w} &= \frac{\partial Z}{\partial \dot w} = -C_{L\dot w}\tfrac{1}{2}\rho SC_a
\end{aligned} \tag{6}$$

$$\begin{aligned}
M_w &= \frac{\partial M}{\partial w} = C_{mw}\tfrac{1}{2}\rho SVC_a \\
M_q &= \frac{\partial M}{\partial q} = C_{mq}\tfrac{1}{2}\rho SVC_a^2 \\
M_{\dot w} &= \frac{\partial M}{\partial \dot w} = C_{m\dot w}\tfrac{1}{2}\rho SC_a^2\,.
\end{aligned} \tag{7}$$

The dimensionless stability derivatives were defined and computed from the following formulae:

$$\begin{aligned}
&C_{Du} = C_{L\dot w} \cong 0\,, \\
&C_{Dw} = \frac{\partial C_D}{\partial\left(\frac{w}{V}\right)} = \frac{2C_L}{\pi A}a + \frac{2C_{LH}}{\pi A_H}a_1\left(1 - \frac{\partial\varepsilon}{\partial\alpha}\right)\frac{S_H}{S}\,, \\
&C_{Dq} = \frac{\partial C_D}{\partial\left(\frac{qC_a}{V}\right)} = \frac{2C_{LH}}{\pi A_H}a_1\kappa_H\,,
\end{aligned} \tag{8}$$

where $\kappa_H = \dfrac{S_H(x_{AH} - x_C)}{SC_a}$

and

$$C_{Lu}=C_{mu}\cong 0$$

$$C_{Lw}=\frac{\partial C_L}{\partial\left(\frac{w}{V}\right)}=a+a_1\left(1-\frac{\partial\varepsilon}{\partial\alpha}\right)\frac{S_H}{S}$$

$$C_{Lq}=\frac{\partial C_L}{\partial\left(\frac{qC_a}{V}\right)}=a_1\kappa_H\left(\frac{V_H}{V}\right)^2 \qquad (9)$$

$$C_{L\dot{w}}=\frac{\partial C_L}{\partial\left(\frac{\dot{w}C_a}{V^2}\right)}=a_1\frac{\partial\varepsilon}{\partial\alpha}\kappa_H\left(\frac{V_H}{V}\right)^2$$

$$C_{mw}=\frac{\partial C_m}{\partial\left(\frac{w}{V}\right)}$$

$$=a\left(\frac{\partial C_{mwB,C}}{\partial C_L}-\frac{a_1}{a}\left(1-\frac{\partial\varepsilon}{\partial\alpha}\right)\kappa_H\left(\frac{V_H}{V}\right)^2\right) \qquad (10)$$

$$C_{mq}=\frac{\partial C_m}{\partial\left(\frac{qC_a}{V}\right)}=-\frac{\pi}{8}-a_1\kappa_H\left(\frac{V_H}{V}\right)^2\frac{x_{AH}-x_C}{C_a}$$

$$C_{m\dot{w}}=\frac{\partial C_m}{\partial\left(\frac{\dot{w}C_a}{V^2}\right)}=-a_1\frac{\partial\varepsilon}{\partial\alpha}\kappa_H\left(\frac{V_H}{V}\right)^2\frac{x_{AH}-x_C}{C_a}\,.$$

The dimensionless, longitudinal stability derivatives depend on lift coefficient C_L, steady angle of attack α_{ST} and airplane speed $V=V_\infty$. The X-2000 airplane at speed $V=100$ m/s has the following stability derivatives (Tab.1):

Tab.1 Values of dimensionless stability derivatives

derivative	numerical value
$C_{Dw}=\frac{\partial C_D}{\partial\left(\frac{w}{V}\right)}$	0.749
$C_{Dq}=\frac{\partial C_D}{\partial\left(\frac{qC_a}{V}\right)}$	0.0821
$C_{Lw}=\frac{\partial C_L}{\partial\left(\frac{w}{V}\right)}$	4.03
$C_{Lq}=\frac{\partial C_L}{\partial\left(\frac{qC_a}{V}\right)}$	1.19
$C_{L\dot{w}}=\frac{\partial C_L}{\partial\left(\frac{\dot{w}C_a}{V^2}\right)}$	0.562
$C_{mu}=\frac{\partial C_m}{\partial\left(\frac{u}{V}\right)}$	0.14
$C_{mw}=\frac{\partial C_m}{\partial\left(\frac{w}{V}\right)}$	-0.707
$C_{mq}=\frac{\partial C_m}{\partial\left(\frac{qC_a}{V}\right)}$	-1.75
$C_{m\dot{w}}=\frac{\partial C_m}{\partial\left(\frac{\dot{w}C_a}{V^2}\right)}$	-0.562

The dynamic equations of motion can be rewritten in the matrix form

$$\mathbf{M}\dot{\mathbf{x}}=\mathbf{B}\,, \qquad (11)$$

where

$$\mathbf{M}=\begin{bmatrix} m & 0 & 0\\ 0 & m-Z_{\dot{w}} & 0\\ 0 & -M_{\dot{w}} & J_y\end{bmatrix}, \qquad (12)$$

$$\mathbf{B}=\begin{bmatrix} \Delta X+X_u u+X_w w+X_q q+X_{\dot{w}}\dot{w}\\ +mg(\cos\Theta_0\sin\vartheta)-mqW_0-mqw\\ \Delta Z+Z_u u+Z_w w+Z_q q+Z_{\dot{w}}\dot{w}\\ -mg(\sin\Theta_0\sin\vartheta)+mqU_0+mqu\\ \Delta M+M_u u+M_w w+M_q q+M_{\dot{w}}\dot{w}\end{bmatrix}. \qquad (13)$$

4 Aircraft used for testing

The approach used in this paper enables computing the unsteady aerodynamic and inertial forces acting on the airplane structure, then finally the extreme states of loads. The detailed calculations were performed for X-2000 subsonic jet trainer airplane, designed and assembled in a small private company in Poland, now under the flight tests. Configuration (Fig.1) reminds the Falcon

version of Bede BD-10 light aircraft, however X2000 is an original new concept aerodynamically designed from scratch. It is a tandem two-seat, subsonic, fully composite airplane, wings with leading edge sweepback, twin fins and rudders, non-boosted dual controls, retractable tricycle type landing gear, take-off mass equal to 2400 kg, one turbojet engine of 13 kN thrust.

Control surface deflections were of the step change type, gust was assumed to be either of the step change type or harmonic, with a gust cycle time corresponding to the time to travel a distance equal to 25 *MAC* [4]. In all cases a jump type elevator deflection was assumed to last for 1 s, whilst the airplane response was observed for 3 s. The airplane motion and loads acting on the tailplane and main wing were calculated by means of numerical integration.

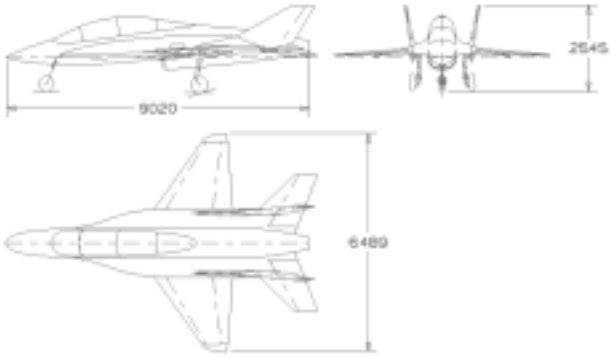

Fig.1 X-2000 - light subsonic jet trainer

5 Influence of altitude on gust maneuver

All maneuvers considered here are computed under the assumption that they are performed at Sea Level. An increment in the dynamic angle of attack is equal to

$$\Delta\alpha = \frac{W_g - W}{V} = \frac{W_g}{V}\left(1 - \frac{W}{W_g}\right) . \qquad (14)$$

A simple model of one degree of freedom can be used to calculate the vertical speed *W*. This model has the form of a linear differential equation

$$m\dot{W} = \tfrac{1}{2}\rho V^2 S \frac{W_g - W}{V} C_{L\alpha} , \qquad (15)$$

and it can be rewritten as follows:

$$m\dot{W} + qS\frac{C_{L\alpha}}{V}W = qS\frac{C_{L\alpha}}{V}W_g . \qquad (16)$$

The solution of eq. (16) has the form:

$$\frac{W}{W_g} = \left(1 - e^{-\frac{qSC_{L\alpha}}{mV}t}\right) , \qquad (17)$$

and it is presented in Fig.2 as a function W/W_{gust} versus time.

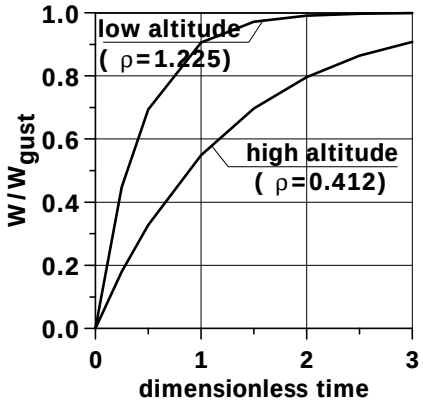

Fig.2 Vertical speed versus time, depending on the flight altitude

From this analysis it follows that the higher altitude the higher normal load coefficient and the more severe maneuver (under the assumption that speed *V* and the lift-curve slope ($a = \partial C_{Lw}/\partial\alpha$) do not change with altitude). The above conclusion can be written in the form:

Low altitude ⇒ high ρ ⇒ high W/W$_g$ ⇒ small Δα ⇒ small ΔL ⇒ small n

6. Results and discussion

Tab.2 Three differently-defined angles of attack: α_{ST}, α_{DYN}, α_{KIN}

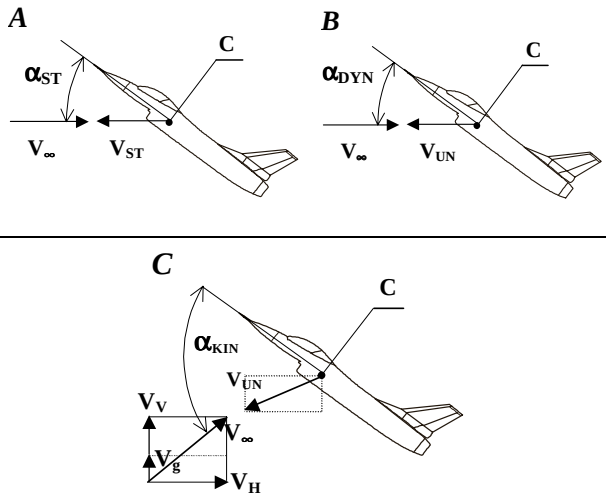

One has to emphasize the differences between a flight analysis, including and excluding gust. In the case when gust is not included (both either in a steady flight (case A) or unsteady flight (case B)) vectors of speed of the center of gravity V_{ST} or V_{UN}, and the corresponding vectors of air-flow over the airplane V_∞, have the same values and are opposite in direction. In the case when gust is included (case C) both vectors are completely different, i.e. they are out-of-parallel and can have different lengths. All these vectors and corresponding angles of attack are shown in Tab.2.

A number of selected maneuvers has been presented and discussed in [7,9,10]. The dynamic response of the X-2000 airplane following either a sudden elevator deflection or gust has been computed for three basic cases [7,9].

The first case corresponds to a sudden elevator deflection of the step change type and is shown in Fig.3-6. Fig.3 shows the increments of longitudinal *(ΔU)* and vertical *(ΔW)* speeds, elevator deflections δ_H , kinematic angle of attack α_{kin} (angle between vector of the air-flow over the airplane and *MAC* direction), dynamic angle of attack $\alpha = \alpha_{dyn}$ (angle between vector of the airplane speed and *MAC* direction) and the normal load coefficient n_Z .

In order to investigate a sensitivity of the airplane dynamic response to the speed of elevator motion a number of the elevator control functions have been defined and used in simulations [13,14]. Among these control functions there are an exponential function and two damped, harmonic-type functions (one of them corresponds to a lower-frequency-deflection and second corresponds to higher-frequency-deflection). These functions are defined as follows:

- exponential function

$$\delta_H = \delta_{H0}\left\{1 - e^{-(kt)^2}\right\} \quad if \quad t \le t_k \; ; \qquad (18)$$

and

$$\delta_H = \delta_{H0}\left\{1 - e^{-(k[t-t_k])^2}\right\} \quad if \quad t > t_k \; ; \qquad (19)$$

where t_k – instant of time, after which elevator deflection decreases to its initial value; k – a positive constant; δ_{H0} – amplitude of elevator deflection;

- harmonic-type function (higher-frequency-deflection)

$$\delta_H = \delta_{H0}\sin(\omega t)e^{-2t}\frac{1}{s} \; ; \; \omega = 0.5 * 2\pi \; ; \qquad (20)$$

- harmonic-type function (lower-frequency-deflection)

$$\delta_H = \delta_{H0}\sin(\omega t)e^{-2t}\frac{1}{s} \; ; \; \omega = 0.3 * 2\pi \quad ; \qquad (21)$$

where

$$s = \sin(\omega x)e^{-2x} \quad whilst \quad x = \frac{\tan^{-1}\left(\frac{\omega}{2}\right)}{\omega} \; . \qquad (22)$$

Fig.4-5 (similarly as Fig.3) present the increments of longitudinal *(ΔU)* and vertical *(ΔW)* speeds, kinematic angle of attack α_{kin}, dynamic angle of attack α (i.e. the current angle of attack) and the normal load coefficient n_Z - all these parameters induced by the elevator deflections δ_H of harmonic-type, either higher or lower-frequency.

Fig.6 shows a comparison of the time-dependent elevator deflection curves, computed on the basis of formulae (18-22). This figure contains also the corresponding increments of speed, *Δw*. All other parameters change after elevator deflection in the same way, i.e. they are not sensitive to the type of function describing the elevator deflection.

The case number two (Fig.7-9) relates to the dynamic response following the gust of the step change type, acting simultaneously either on the whole airplane (Fig.7), or on its selected parts. The worst case (Fig.8) is when the vertical gust (even a small one of 2 m/s) acts on the main wing only. It is involved by the fact that even a small increment in the main wing load (being not compensated on the tailplane) creates a large pitching moment about the mass center, being able to rotate the airplane very rapidly. It could be very dangerous, however such a case is not very likely in a real flight.

The case number three (Fig.10-15) relates to dynamic response following a harmonic gust shape according to the Federal

Aviation Regulations specification [4]. The shape of the gust is given by the following equation:

$$W = \frac{W_0}{2}\left(1 - \cos\frac{2\pi V t}{25c}\right) \quad , \qquad (23)$$

where W_0 - gust velocity amplitude referred to by the Federal Aviation Regulations specification [4], V - flight speed, c - Mean Aerodynamic Chord.

Fig.10-11 show selected airplane responses: α_{KIN} - kinematic angle of attack, α_{DYN} - dynamic (real) angle of attack, ΔW - increment of vertical speed, L_H - aerodynamic tailplane load and n_z - normal load coefficient.

Fig.12-15 compare selected parameters for different gust velocity amplitudes: W_0 = 7.5, 15; -15 & -7.5 m/s. The worst case corresponds to the gust of 15 m/s and it means that the tailplane load can increase more than 4 times in comparison to the static load case. The obtained results can be further used for the strain and fatigue analysis.

6. Conclusion

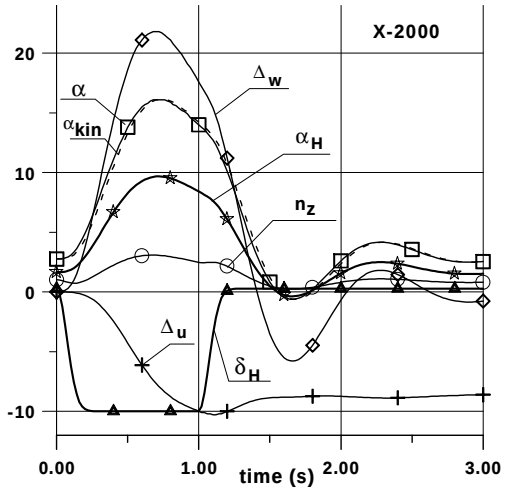

Fig.3 Selected kinematic and dynamic parameters versus time following the elevator deflection according to exponential function

It was found that the most critical state corresponds to the case when the gust acts on the part of airplane only. A great difference arises if the kinematic and dynamic angles of attack differ between themselves. Dynamic angle of attack (α_{dyn}) for gust acting up is lower than that of the kinematic (α_{kin}) and its curve-course is delayed with respect to α_{kin}. Otherwise, the dynamic angle of attack (α_{dyn}) is higher (for gust acting down) than the kinematic angle of attack (α_{kin}) and its curve-course is also delayed with respect to α_{kin}. Dynamic response is very sensitive to the amplitude of elevator deflection and is not sensitive with respect to the speed of elevator deflection – only an increment of vertical speed depends slightly on the type of elevator motion and only over a limited time, very short period of time. During a severe gust the dynamic tailplane force can be several times greater than that in a steady level flight.

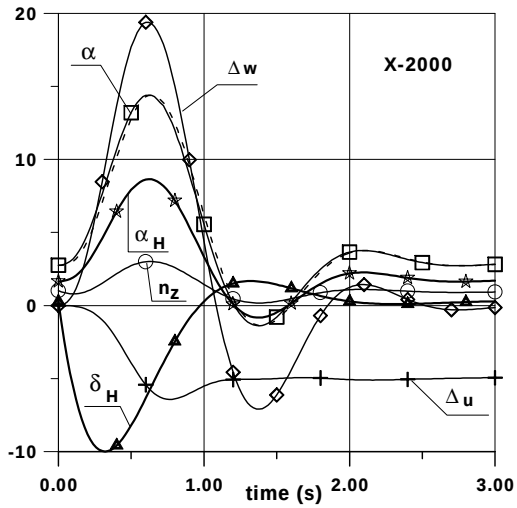

Fig.4 Selected kinematic and dynamic parameters versus time following the elevator deflection according to a harmonic-type function (higher-frequency-deflection)

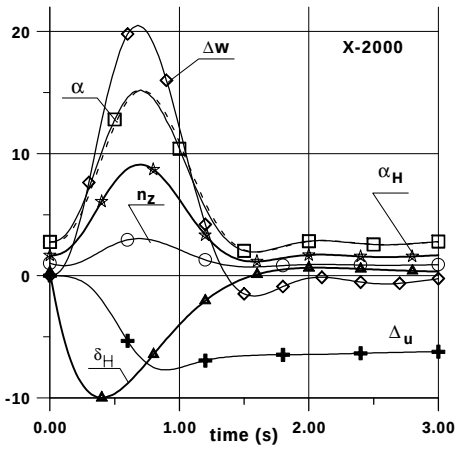

Fig.5 Selected kinematic and dynamic parameters versus time following the elevator deflection according to a harmonic-type function (lower-frequency-deflection)

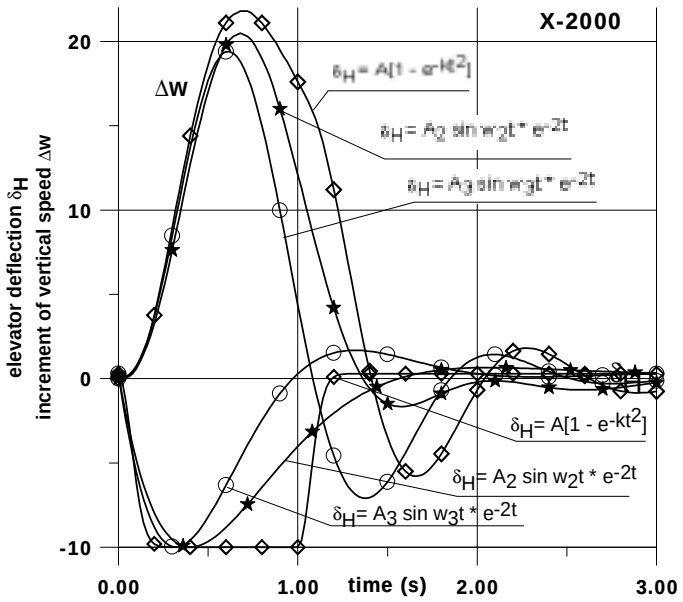

Fig.6 Three different functions of elevator deflection δ_H (exponential, lower-frequency-harmonic-type and higher-frequency-harmonic-type) and corresponding disturbances of vertical speed ΔW

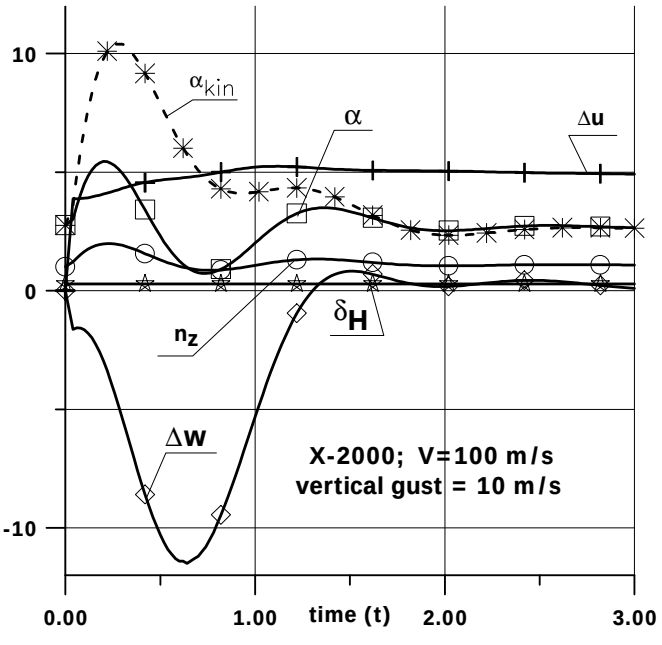

Fig.7 Dynamic response of X-2000 airplane following a gust of the step change type (acting on the whole airplane)

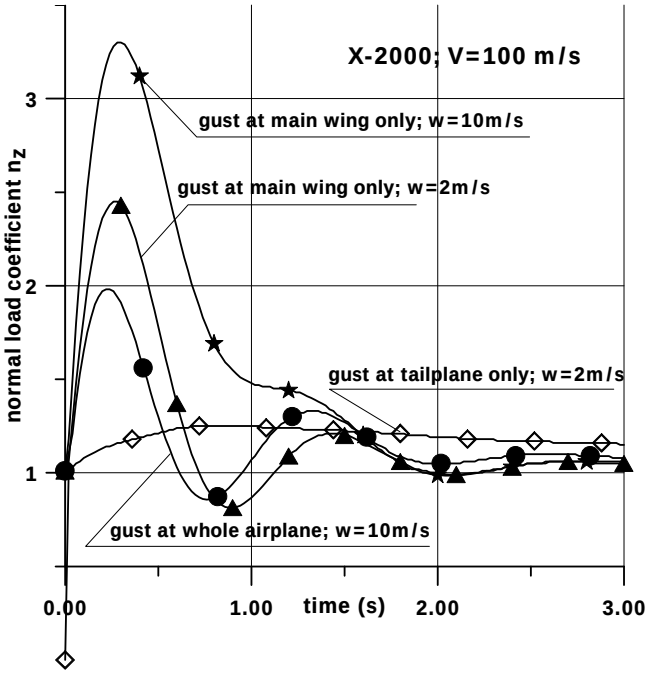

Fig.8 Normal load coefficient following a gust of the step change type (acting on the main wing, or on the tailplane or on the whole airplane)

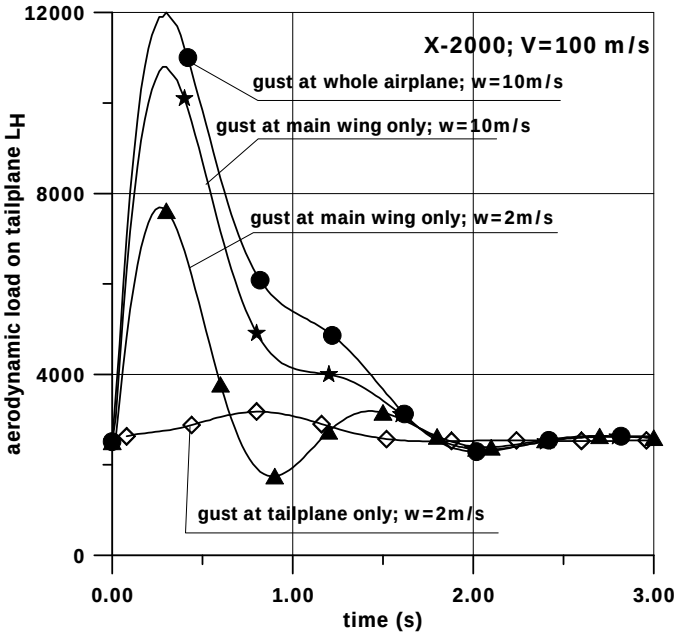

Fig.9 Aerodynamic tailplane load following a gust of the step change type (acting on the main wing, or on the tailplane or on the whole airplane)

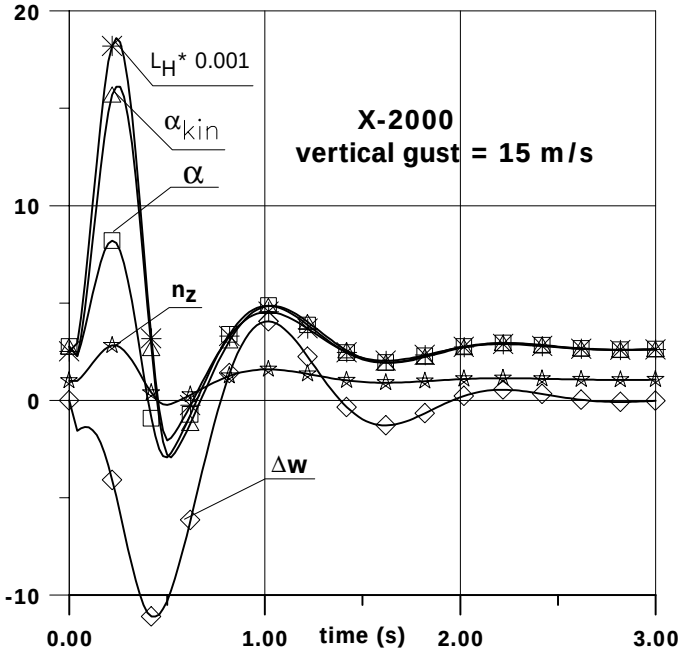

Fig.10 Dynamic response of the X-2000 airplane following vertical gust of the harmonic shape (gust amplitude is equal to 15 m/s)

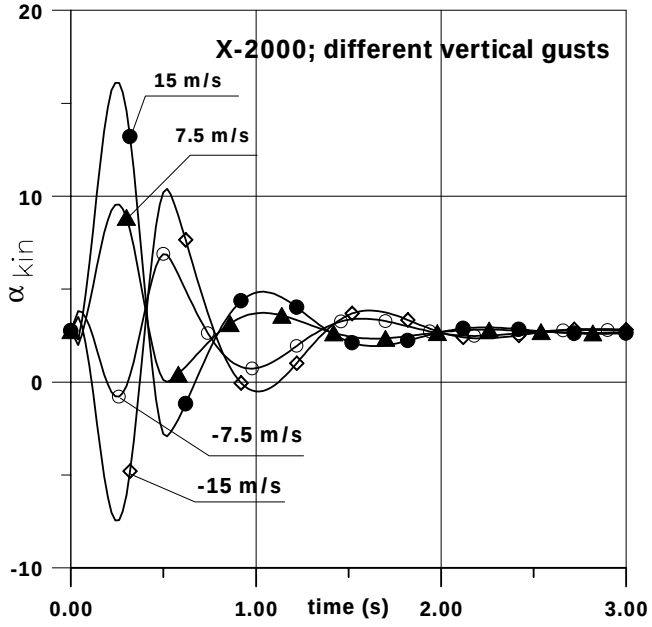

Fig.12 Kinematic angle of attack following vertical gust of the harmonic shape with different amplitudes

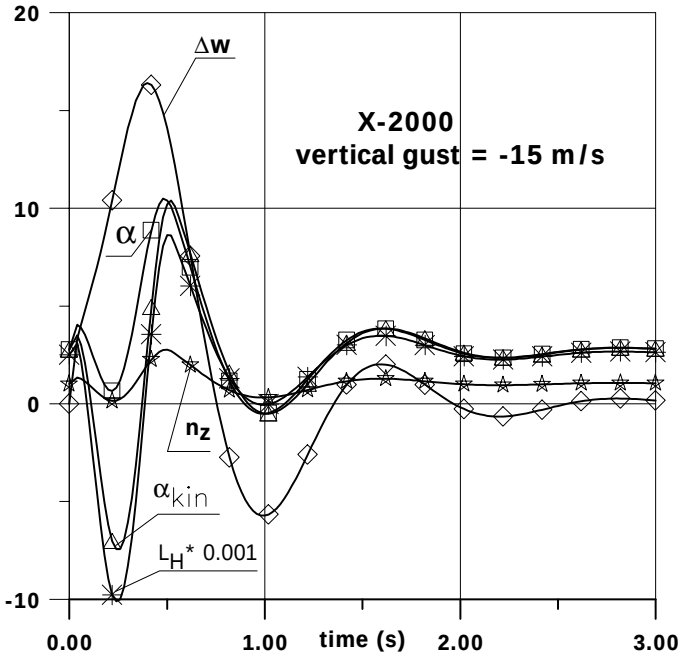

Fig.11 Dynamic response of the X-2000 airplane following vertical gust of the harmonic shape (gust amplitude is equal to -15 m/s)

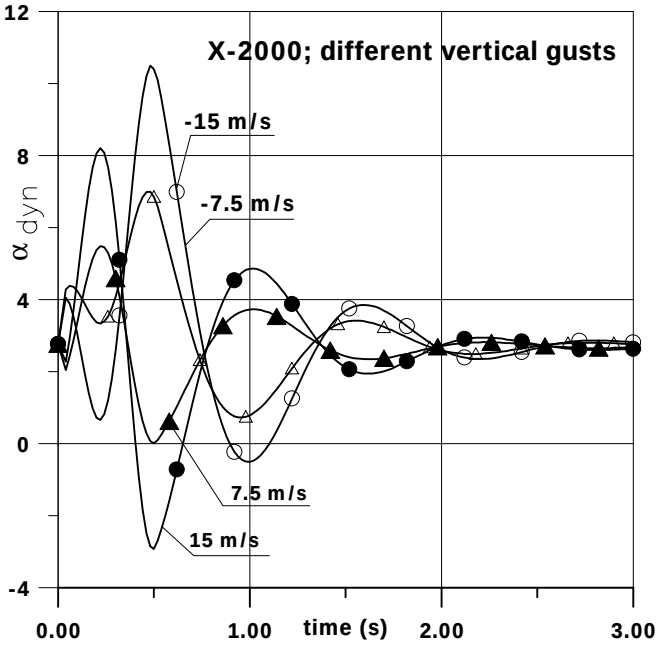

Fig.13 Dynamic angle of attack following vertical gust of the harmonic shape with different amplitudes

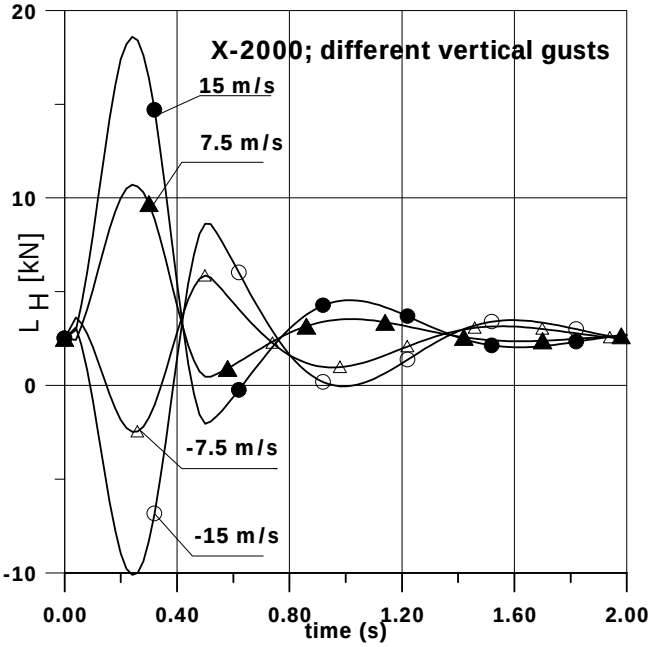

Fig.14 Aerodynamic tailplane force as a function of time following vertical gust of the harmonic shape with different amplitudes

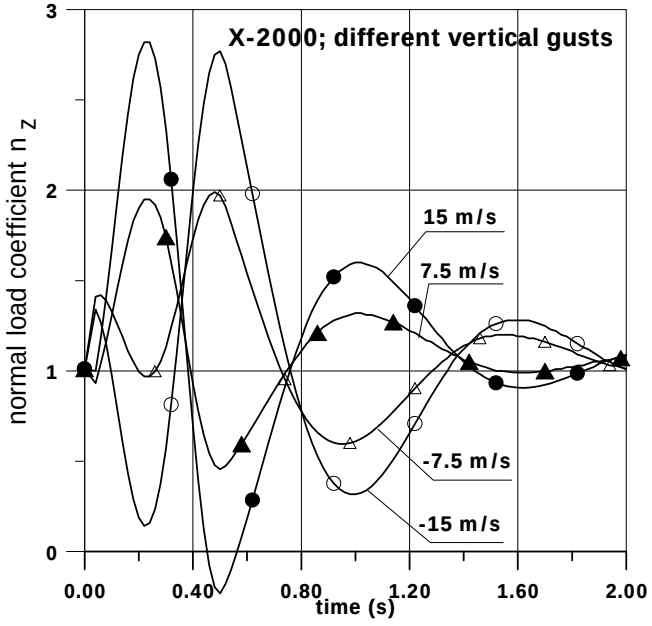

Fig.15 Normal load coefficient as a function of time following vertical gust of the harmonic shape with different amplitudes

8 References

[1] Bertin J.J., Smith M.L. *Aerodynamics for Engineers, Prentice-Hall International*, Inc. London 1989.

[2] Cook M.V. *Flight dynamics principles.* 1st edition, Arnold, 1997.

[3] *ESDU - Engineering Sciences Data Unit, Sub-series Aerodynamics*, 3A, Regent Street, London W1R 7AD, England (ESDU - Data Sheets).

[4] *FAR - Federal Aviation Regulations*, Part 23, Federal Aviation Administration Superintendent of Documents, US Government Printing Office.

[5] Goraj Z., Kulicki P., Lasek M. Aircraft stability analysis for strongly coupled aerodynamic configuration. *Journal of Theoretical & Applied Mechanics.* Vol.35, 1, pp.137-158, 1997.

[6] Goraj Z., Pietrucha J. Basic Mathematical Relations of Fluid Dynamics for Modified Panel Methods. *Journal of Theoretical & Applied Mechanics.* Vol.36, 1, pp. 47-66, 1998.

[7] Goraj Z., Sznajder J. Rapport BP/39/99 at Institute of Aviation: Manoeuvring Loads on M-28 Aircraft Tailplane Computed for Fatigue Test, Warsaw, Oct.1999, unpublished.

[8] Goraj Z. Dynamics of High Altitude Long Endurance UAV, ICAS Congress 2000, paper no 362, 10 pages, Sept. 2000, Haroggate, England.

[9] Goraj Z., Sznajder J. Extreme Load Calculation Following a Sudden Elevator Deflection or Vertical Gust, *Proceedings of the Fourth International Seminar: Recent Research and Design Progress in Aeronautical Engineering and its Influence on Education.* Warsaw University of Technology, Bul. No 10, Warsaw 2000, pp.121-130.

[10] Goraj Z., Sznajder J. Extreme loads acting on transport airplane following a sudden change in symmetric equilibrium. *Aircraft Engineering and Aerospace Technology - An International Journal*, 2002 (in the press).

[11] Hess J. L., Smith A. M. O. Calculation of potential flow about arbitrary bodies, *Progress in Aeronautical Sciences*, Vol.8, (Ed. D.Küchemann), Pergamon Press, Oxford, pp.1-138, 1967.

[12] Katz J., Plotkin A. *Low-speed aerodynamics - from wing theory to panel methods.* McGraw-Hill, Inc., New York 1991.

[13] Pearson H.A. Derivation of charts for determining the horizontal tail load variation with any elevator motion, NACA Rep. No 759, Washington DC.

[14] Pearson H.A., Mc Gowan W.A., Donegan J.J. Horizontal tail load in maneuvering flight, NACA Rep. No 759, Washington DC.